Novel ⟨110⟩-Oriented Organic−Inorganic Perovskite Compound Stabilized by *N*-(3-Aminopropyl)imidazole with Improved Optical Properties

Y. Y. Li,[†] C. K. Lin,[†] G. L. Zheng,[†] Z. Y. Cheng,[‡] H. You,[‡] W. D. Wang,[§] and J. Lin*[,†]

Key Laboratory of Rare Earth Chemistry and Physics, State Key Laboratory of Polymer Physics and Chemistry, and State Key Laboratory of Electroanalytical Chemistry, Changchun Institute of Applied Chemistry, Chinese Academy of Sciences, Changchun 130022, People's Republic of China, and Graduate School of the Chinese Academy of Sciences, Beijing 100049, People's Republic of China

Received March 25, 2006. Revised Manuscript Received April 29, 2006

In the organic−inorganic perovskites family, the ⟨100⟩-oriented type has been extensively investigated as a result of its unique magnetic, optical, and electrical properties, and only one type of ⟨110⟩-oriented hybrid perovskite stabilized by methylammonium and iodoformamidinium cations or the latter themselves has been known so far. In this paper, another novel ⟨110⟩-oriented organic−inorganic perovskite $(C_6H_{13}N_3)$-$PbBr_4$ (compound **1**) has been prepared by reacting *N*-(3-aminopropyl)imidazole (API) with $PbBr_2$ in hydrobromic acid. The crystal structure is determined, which indicates that the perovskite is stabilized by API. The introduction of the optically active organic ligand API into the hybrid perovskite results in a red shift and a great enhancement of photoluminescence in the perovskite with respect to organic ligand API itself. These results have been explained according to calculation based on density-functional theory. Moreover, the excellent film processing ability for the perovskite $(C_6H_{13}N_3)PbBr_4$ together with the improved optical properties makes it have potential application in optoelectronic devices.

I. Introduction

Organic−inorganic perovskites have attracted much attention because of their unique magnetic,[1] optical,[2] thermochromic,[3] and electrical properties[4] and structure flexibility.[5] In general, this type of hybrid perovskites forms layered structures consisting of sheets of corner-sharing metal halide octrahedra separated by monolayers or bilayers of organic cations (usually primary ammonium). The choice of organic cations in this structure can both control the dimensionality of the inorganic sheets and influence the crystallographic orientation of the inorganic framework. In this way, physical properties of perovskites are modulated.[5] Most of the organic moieties used in the construction of ammonium salt−metal halide perovskites have been nonfunctional groups such as alkyl chains that play a secondary role of merely helping to improve the processability of the hybrids.[1a] Hybridization of functional organic molecules with perovskites may generate new materials with novel properties.[2e] A good example for this case can also be seen in the recent publication by Tang and co-workers, who introduced the polyacetylenes into the lead bromide perovskite hybrids that have enhanced light emission efficiency.[6]

On the other hand, among the organic−inorganic perovskites the ⟨100⟩-oriented type has been extensively investigated,[1] and few with other orientations have been reported so far.[5a,7] Accordingly, the syntheses of organic−inorganic perovskites with different orientations will continue to be an attractive area of research. A series of ⟨110⟩-oriented organic−inorganic perovskites with composition $[NH_2C(I)=NH_2]_2(CH_3NH_3)_mSn_mI_{3m+2}$ ($m = 1-4$) were reported by Mitzi and co-workers.[7a−c] These perovskites were stabilized by the cooperation of methylammonium and iodoformamidinium cations or the latter themselves. With the increasing of the *m* value, they undergo a semiconductor−metal transition.[7a]

* Corresponding author. E-mail: jlin@ciac.jl.cn.
[†] Key Laboratory of Rare Earth Chemistry and Physics.
[‡] State Key Laboratory of Polymer Physics and Chemistry.
[§] State Key Laboratory of Electroanalytical Chemistry.

(1) (a) Mitzi, D. B. *Prog. Inorg. Chem.* **1999**, *48*, 1. (b) Christopher, P. L.; Kris, E. H.; Willet, R. D. *J. Appl. Phys.* **1987**, *61*, 3295. (c) Willett, R.; Place, H.; Middleton, M. *J. Am. Chem. Soc.* **1988**, *110*, 8639. (d) Long, G. S.; Wei, M.; Willett, R. D. *Inorg. Chem.* **1997**, *36*, 3102.
(2) (a) Ishihara, T.; Takahashi, J.; Goto, T. *Phys. Rev. B* **1990**, *42*, 11099. (b) Hong, X.; Ishihara, T.; Nurmikko, A. V. *Phys. Rev. B* **1992**, *45*, 6961. (c) Mitzi, D. B. *Chem. Mater.* **1996**, *8*, 791. (d) Mitzi, D. B.; Dimitrakopoulos, C. D.; Kosbar, L. L. *Chem. Mater.* **2001**, *13*, 3728. (e) Mitzi, D. B.; Chondroudis, K.; Kagan, C. R. *Inorg. Chem.* **1999**, *38*, 6246. (f) Cheng, Z. Y.; Gao, B. X.; Pang, M. L.; Wang, S. Y.; Han, Y. C.; Lin, J. *Chem. Mater.* **2003**, *15*, 4705. (g) Chondroudis, K.; Mitzi, D. B. *Chem. Mater.* **1999**, *11*, 3028. (h) Era, M.; Oka, S. *Thin Solid Films* **2000**, *376*, 232.
(3) (a) Blinc, R.; Burgar, M. I.; Rutar, V.; Zeks, B.; Kind, R.; Arend, H.; *Phys. Rev. Lett.* **1979**, *43*, 1679. (b) Willett, R. D.; Haugen, J. A.; Lebsack, J.; Morrey, J. *Inorg. Chem.* **1974**, *13*, 2510.
(4) (a) Mitzi, D. B.; Chondroudis, K.; Kagan, C. R. *IBM J. Res. Dev.* **2001**, *45*, 29. (b) Mitzi, D. B.; Feild, C. A.; Harrison, W. T. A.; Guloy, A. M.; *Nature* **1994**, *369*, 467. (c) Mitzi, D. B.; Liang, K. *J. Solid State Chem.* **1997**, *134*, 376. (d) Xiao, Z. L.; Chen, H. Z.; Shi, M. M.; Wu, G.; Zhou, R. J.; Yang, Z. S.; Wang, M.; Tang, B. Z. *Mater. Sci. Eng. B* **2005**, *117*, 313.
(5) (a) Mitzi, D. B.; *J. Chem. Soc., Dalton Trans.* **2001**, 1. (b) Mitzi, D. B. *Chem. Mater.* **2001**, *13*, 3283. (c) Mitzi, D. B. *J. Mater. Chem.* **2004**, *14*, 2355.
(6) Hua, J.; Li, Z.; Lam, J. W. Y., Xu, H.; Sun, J.; Dong, Y.; Dong, Y.; Qin, A.; Yuan, W.; Chen, H.; Wang, M.; Tang, B. *Macromolecules* **2005**, *38*, 8127.
(7) (a) Mitzi, D. B.; Wang, S.; Feild, C. A.; Chess, C. A.; Guloy, A. M.; *Science* **1995**, *267*, 1473. (b) Wang, S.; Mitzi, D. B.; Feild, C. A.; Guloy, A. *J. Am. Chem. Soc.* **1995**, *117*, 5297. (c) Mitzi, D. B.; Liang, K.; Wang, S.; *Inorg. Chem.* **1998**, *37*, 321. (d) Guan, J.; Tang, Z.; Guloy, A. M. *Chem. Commun.* **1999**, 1833.

10.1021/cm060714u CCC: $33.50
Published on Web 06/22/2006

Scheme 1. Growth and Formation Processes for the Organic−Inorganic Perovskite $(C_6H_{13}N_3)PbBr_4$ (a) and API·2HBr (b) Crystals

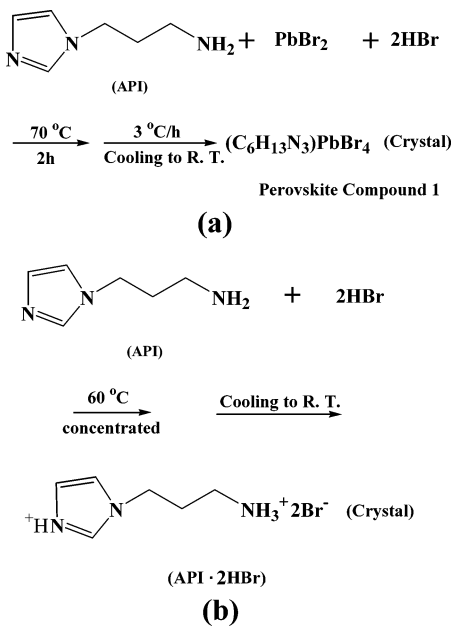

In above examples, the iodoformamidinium cations play an important role in forming ⟨110⟩-oriented hybrid perovskites as a result of their special structures. Since then no other ⟨110⟩-oriented hybrid perovskite has been reported. Accordingly, it is worth exploring other organic ammonium cations that might stabilize the ⟨110⟩-oriented perovskite structure with novel physical properties.

The substituted imidazoles and their derivatives are a kind of optically active organic compound which have tunable fluorescent properties dependent on the solvents and pH values.[8] In this work we report another ⟨110⟩-oriented hybrid perovskite which is stabilized by the optically active organic ligand *N*-(3-aminopropyl)imidazole (API, for molecular structure, see Scheme 1). Other considerations for choosing this organic ligand are as follows. First, it possesses a primary amine on one end which usually can be used to construct perovskite structure; second, it has an imidazole (equal to ternary amine) on the other end which has steric hindrance for the formation of perovskite (usually leading to the formation of metal halide columnar stacks or chains.[9] The two different amine heads on both ends of one organic ligand may lead to novel distorted perovskite. It is found that reaction of API ligand with $PbBr_2$ in acid solution yields a ⟨110⟩-oriented organic−inorganic perovskite $(C_6H_{13}N_3)PbBr_4$ (compound **1**). The structure and photoluminescent (PL) properties of the hybrid perovskite were studied. It is of great interest to find an energy transfer from the inorganic $PbBr_4^{2-}$ sheets (exitons) to the organic component, API·$2H^+$ (API forms a dication in acid solution which is denoted as API·$2H^+$, Scheme 1), and great enhancement of the emission intensity with respect to the ammonium salt, API·2HBr itself. Furthermore, the hybrid perovskite family is suitable for forming a thin film which is essential for device application by a number of simple processing techniques.[10] The ⟨110⟩-oriented perovskite we obtained contains two components only (API·2HBr and a $PbBr_2$ part) instead of three in the known ⟨110⟩-oriented perovskites described by Mitzi et al. (methylammonium, iodoformamidinium, iodostannate),[7] which is an advantage to prepare thin films using the spin-coating technique.

II. Experimental Section

Materials and Syntheses. API (98%, Aldrich), $PbBr_2$ (99.999%, Aldrich), and HBr (≥40%, Beijing Chemical Industry Co., Ltd.) were used as received. A single crystal of compound **1** was obtained in a N_2 atmosphere by heating a mixture of $PbBr_2$ (0.1 mmol), API (0.1 mmol), and HBr (12 mL) to 70 °C and then slowly cooling it (3 °C/h) to room temperature. This organic−inorganic perovskite crystallizes in a monoclinic space group $P2_1/c$.[26] As a comparative control, a single crystal (and powder) of the ammonium salt, API·2HBr, was prepared by evaporating a solution of API dissolved in 40% hydrobromic acid. The growing and formation processes for the organic−inorganic perovskite $(C_6H_{13}N_3)PbBr_4$ and API·2HBr crystals are shown in Scheme 1.

Thin Film Deposition. Thin film of the perovskite compound **1** was prepared by spin coating a *N*,*N*-dimethylformamide (DMF) solution on a quartz substrate. The coating solution was prepared by dissolving 10 mg of recrystallized hybrid perovskite compound **1** in 3 mL of DMF. The film was prepared by flooding the substrate with solution and a spinning cycle with 1 s ramping to 1500 rmp and dwelling for 50 s at 1500 rpm. Then the substrate was heated at 100 °C for 20 min to remove residual solvent.

Characterization. Diffraction intensities for the single crystals of compound **1** and API·2HBr were collected on a Rigaku RAXIS-RAPID image plate diffractometer using the w-scan technique with Mo Kα radiation ($\lambda = 0.071\,07$ nm). Absorption corrections were applied using the multiscan technique.[11] The structures were solved by direct methods using SHELXS-97[12] and refined by means of full-matrix least-squares techniques using the SHELXL-97 program[13] as implemented in WINGX.[14] Non-hydrogen atoms were refined anisotropically. The positions of hydrogen atoms attached to carbon were generated geometrically. Analytical expressions of neutral-atom scattering factors were employed, with anomalous dispersion corrections incorporated therein.[15] The X-ray diffraction (XRD) of the film sample was examined on a Rigaku-Dmax 2500 diffractometer using Cu Kα radiation ($\lambda = 0.154\,05$ nm). The excitation and emission spectra were taken on a Hitachi F-4500 spectrofluorimeter equipped with a 150 W xenon lamp as the excitation source. The morphology of the thin film was measured on an atomic force microscope (AFM, Bermad-2000 SPM) in tapping mode. The band structures of the API ligand and the

(8) (a) Tway, P. C.; Cline Love, L. J. *J. Phys. Chem.* **1982**, *86*, 5227. (b) Tway, P. C.; Cline Love, L. J. *J. Phys. Chem.* **1982**, *86*, 5223.
(9) (a) Willett, R. D.; Maxcy, K. R.; Twamley, B. *Inorg Chem.* **2002**, *41*, 7024. (b) Angeloni, A.; Crawford, P. C.; Orpen, A. G.; Podesta, T. J.; Shore, B. J. *Chem.—Eur. J.* 2004, *10*, 3783. (c) Angeloni, A.; Orpen, A. G. *Chem. Commun.* **2001**, 343.
(10) (a) Liang K.; Mitzi D. B.; Prikas M. T. *Chem. Mater.* **1998**, *10*, 403. (b) Mitzi, D. B.; Prikas, M. T.; Chondroudis, K. *Chem. Mater.* **1999**, *11*, 542.
(11) Higashi, T. *Program for Absorption Correction*; Rigaku Corporation: Tokyo, Japan, 1995.
(12) Sheldrick, G. M. *SHELXS-97, A Program for Automatic Solution of Crystal Structure*; University of Goettingen: Goettingen, Germany, 1997.
(13) Sheldrick, G. M. *SHELXL-97, A Program for Crystal Structure Refinement*; University of Goettingen, Goettingen, Germany, 1997.
(14) Farrugia, L. J. *WINGX, A Windows Program for Crystal Structure Analysis*; University of Glasgow: Glasgow, U.K., 1988.
(15) Cromer, T. *International Tables for X-ray Crystallography*; Kluwer Academic: Dordrecht, 1992; Vol. C.

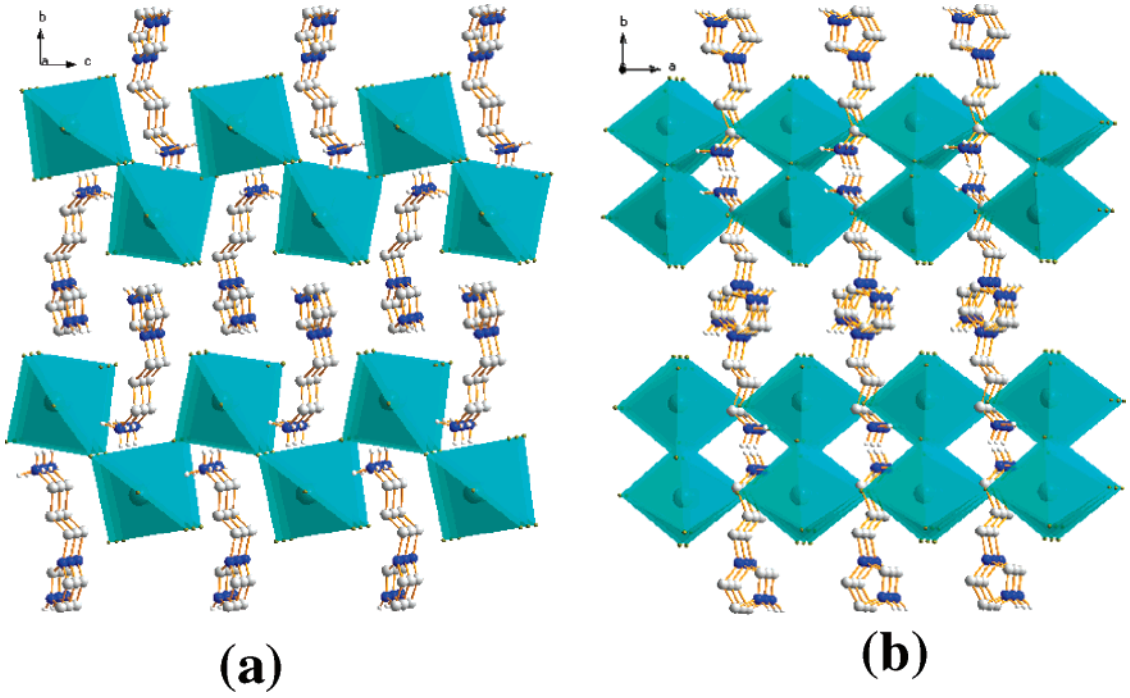

Figure 1. Crystal structure of perovskite compound **1** viewed down the *a* axis ⟨100⟩ (a) and *c* axis ⟨001⟩ (b).

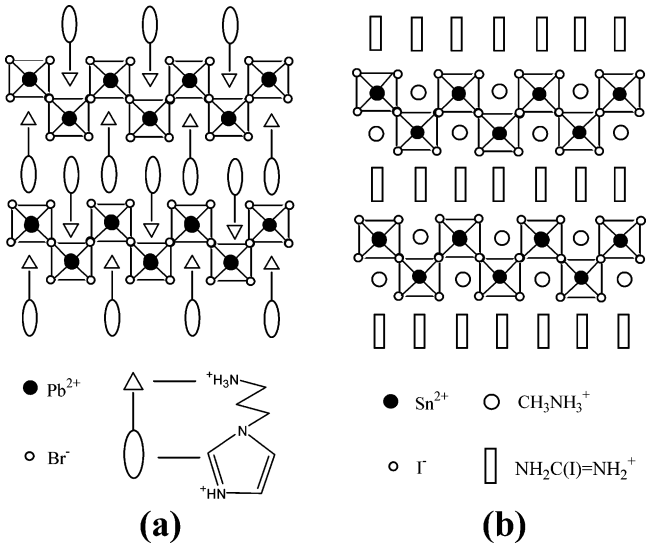

Figure 2. Comparison of the structure of compound **1** (a) with the previously reported ⟨110⟩-oriented perovskite $[NH_2C(I)=NH_2]_2(CH_3NH_3)_2Sn_2I_8$ (b, Mitzi et al.[7a]).

perovskite were calculated using the CASTEP code (version 3.0, Accelrys) based on the density-functional theory (DFT).

III. Result and Discussion

Structure Description. Figure 1 shows the structure of the compound **1** viewed down the ⟨100⟩ (Figure 1a) and ⟨001⟩ (Figure 1b) orientations, respectively. Compared with the reported series $[NH_2C(I)=NH_2]_2(CH_3NH_3)_mSn_mI_{3m+2}$ (m = 1−4),[7a−c] it can be concluded that compound **1** is a ⟨110⟩-oriented hybrid perovskite. As a representative example, a comparison of the structure of compound **1** (Figure 2a) with the previously reported ⟨110⟩-oriented perovskite $[NH_2C(I)=NH_2]_2(CH_3NH_3)_2Sn_2I_8$ (m = 2; Figure 2b) is shown Figure 2. Different from the previously reported ⟨110⟩-oriented perovskites,[7a] in the present case the function of the iodoformamidinium and methylammonium cations in $[NH_2C(I)=NH_2]_2(CH_3NH_3)_2Sn_2I_8$ is merged into the two parts of one single dication of API·$2H^+$. Compared with $[NH_2C(I)=NH_2]_2(CH_3NH_3)_2Sn_2I_8$,[7a] it can be seen that the API·$2H^+$ dications replace the methylammonium and iodoformamidinium cations and have similar function to the two cations on formation of perovskite sheets. The primary ammonium (N1) on one head may be regarded as the methylammonium, while the imidazolium (N3) on the other head seems to take an effect similar to that of the iodoformamidinium. Such structure of the organic dication brings about the formation of the ⟨110⟩-oriented perovskite sheets. It is the unprecedented one single dication that builds up a layered ⟨110⟩-oriented perovskite.

In Figure 1a for the structure of compound **1** viewed along the *a* axis, the lead bromine octrahedra in this compound take a slightly distorted configuration with Br−Pb−Br angles ranging from 86.35 to 96.42° and Pb−Br bond lengths ranging from 2.788 to 3.261 Å, respectively. This indicates that the lone pair electrons of lead(II) are stereochemically active.[7b] Within a given sheet, the $PbBr_2$ octrahedra share neighboring corners (Br4) extending down the crystallographic *c* axis and opposite corners (Br1) along the *a* axis (Figure 3), which build up zigzag perovskite sheets in the *ac* plane. Neighboring sheets are held together by the organic dication API·$2H^+$. In these ⟨110⟩-oriented perovskite sheets the angle Pb−Br4−Pb is 162.68° (Figure 3), slightly deviating from the straight angle. This indicates that the adjacent octahedra are slightly rotated relative to each other in the *bc* plane. Along the *a* axis the perovskite sheets also have a slight corrugation with the angle of Pb−Br1−Pb being 171.85°.

The ⟨110⟩-oriented perovskite sheets are stabilized by the interleaved layers of the API·$2H^+$ dications. The dication contains both protonated primary (N1) and ternary (imidazole nitrogen N3) ammonium groups. Two types of different

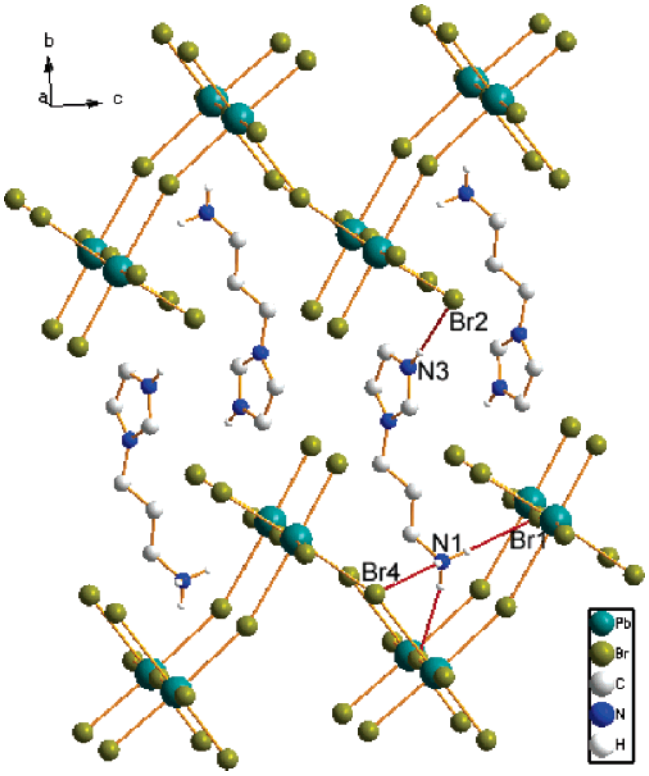

Figure 3. Structure of compound **1** with the atom numbering and hydrogen bonds (shown as red lines).

hydrogen bonds form in this organic-based perovskite structure. On one hand the three hydrogen atoms of the primary ammonium N1 (Figure 3) adopt the bridging halide hydrogen bonding configuration in one sheet;[1a] on the other hand, as a result of the steric hindrance, the hydrogen atom of the imidazolium N3 forms hydrogen bonds with the terminal bromine (Br2) of the neighboring sheet. The two special types of hydrogen bonds together with the electrostatic interactions between the organic cations and inorganic anions stabilize the ⟨110⟩-oriented perovskite sheets to some extent.

Film Morphology. AFM topology images for the spin-coated film of compound **1** are shown in Figure 4. From the planar image (Figure 4a), it can be seen that the film is uniform, consisting of fine and even grains with sizes ranging from 100 to 200 nm. The film surface has a root-mean-square roughness of 83.9 nm, as shown in the stereo image (Figure 4b). The XRD study reveals that the film is well-crystallized and highly oriented, exhibiting well-defined and equal spaced (0*k*0) (*k* = 2, 4, 6, ...) diffraction peaks (Figure 5). The above results indicate that the ⟨110⟩-oriented perovskite compound **1** is easy to processed into thin films, which provides the potential opportunity of using the hybrid material for extensive applications.

Optical Properties. Under longer wavelength ultraviolet (365 nm from a UV lamp) irradiation, the API·2HBr salt shows a very weak blue emission which can only be detected by the spectrophotometer, while the hybrid perovskite compound **1** shows a strong deep yellow emission which can be seen clearly even by the naked eye. Figure 6 shows the PL excitation and emission spectra of the hybrid perovskite (compound **1**) with respect to those of API·2HBr. The emission spectrum of API·2HBr contains a broad band (390−600 nm) with a maximum around 436 nm (Figure 6b), and the corresponding excitation spectrum (Figure 6a) consists of a broad band peaking around 360 nm due to the $\pi-\pi^*$ transitions in API·2HBr.[8] The formation of the hybrid perovskite compound **1** changes the luminescence properties greatly. In Figure 6c for the excitation spectrum of compound **1**, apart from the characteristic absorption band around 360 nm due to the API·$2H^+$ organic ligand component, a strong narrow excitation band at 398 nm is present. This band is the typical exciton absorption arising from the two-dimensional $PbBr_4^{2-}$ layers in organic/inorganic perovskite structure,[16] further confirming the formation of the layered perovskite structure in compound **1**. Upon excitation into the absorption band of the ligand at 360 nm, the obtained emission spectrum consists of a broad band ranging from 400 to 650 nm, with one narrow peak at 424 nm and another broad band peaking at 503 nm, as shown in Figure 6d. The former emission peak (424 nm) is the characteristic exciton emission arising from the two-dimensional $PbBr_4^{2-}$ layers in the perovskite compound **1** with the corresponding excitation peak at 398 nm, and the latter is mainly from the

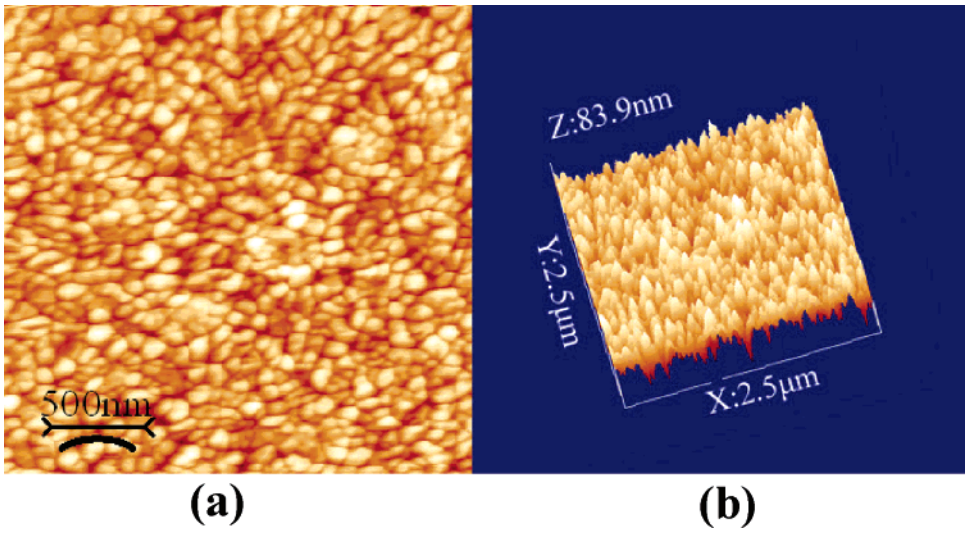

Figure 4. AFM topology planar (a) and stereo (b) images for the spin-coated film of hybrid perovskite compound **1**.

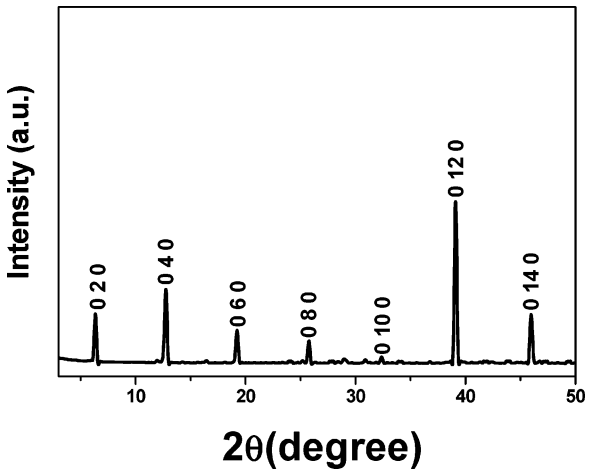

Figure 5. XRD pattern for the thin film of hybrid perovskite compound **1**.

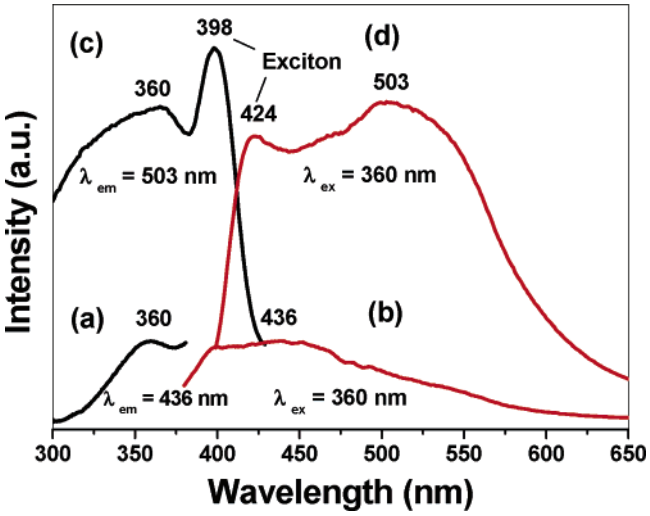

Figure 6. PL excitation (a, c) and emission (b, d) spectra for API·2HBr (a, b) and the perovskite compound **1** (c, d) under the same instrumental conditions.

organic component API·$2H^+$ in the perovskite compound **1**. The small Stokes shift (26 nm) between the PL excitation (398 nm) and emission (424 nm) as well as the narrow bandwidth of the peaks is characteristic of exciton.[16] The perovskite compound **1** can be considered as a semiconductor.[17] Under the excitation of 360 nm irradiation (note that the exciton also has moderate absorption at this wavelength although the maximum is located at 398 nm), an electron (⊖) is excited from the valence band (VB) to the conduction band (CB), leaving a hole (⊕) in the VB. The electron (⊖) and the hole (⊕) move freely in the CB and VB, forming an exciton. The recombination of the electron and hole in the exciton yields an emission around 424 nm.[18]

Furthermore, the integrated emission intensity of the perovskite compound **1** increases greatly (>6 times) with respect to that of the ligand salt API·2HBr under the same excitation condition (λ_{ex} = 360 nm), accompanied by the red shift of the emission maximum (503 nm in the former vs 436 nm in the latter). To explain these changes, the crystal structure of the free ligand API·2HBr was obtained and is shown in Figure S1 (Supporting Information). Compared with the free ligand ammonium API·2HBr crystal, the $\pi-\pi$ stacking interactions among neighboring imidazolium rings in compound **1** increase with the reduced separation of neighboring imidazolium in the perovskite (interplanar distances between two neighboring separate imidazolium ring are 3.823 Å in the free ligand and 3.558 Å in the perovskite, respectively). It is generally thought that the center-to-center distance of $\pi-\pi$ stacking intramolecular interactions ranges from 3.3 to 3.7 Å. Confinement by the hydrogen bonds together with the electrostatic interactions between perovskite sheets in compound **1** leads the arrangement of API dications in the crystal to become more ordered and close. Although a quenching of luminescence may be noticed if quite strong intermolecular interactions occur, some compounds still show fluorescence with a shift to longer wavelength.[19] In the case of the perovskite structure, the increasing $\pi-\pi$ stacking intermolecular interactions of the ammonium ligand in the perovskite lowers the $\pi-\pi^*$ transition energy and brings about the red shift for the emission of API·2HBr.[20]

Fluorescence emission intensity of the imidazole ligand is generally weak. The ligand's contribution to the fluorescence properties of the complex is very limited.[21] The greatly improved emission intensity in the perovskite compound **1** can be attributed to two factors. One comes from the additional contribution to the emission from the excitons, and another is resulted from the energy transfer from the excitons (from two-dimensional $PbBr_4^{2-}$ layers) to the organic ligand API·$2H^+$. This can be seen clearly from the presence of the excitation band of the excitons in the excitation spectrum (Figure 6a) monitored by the emission of the API·$2H^+$ (λ_{em} = 503 nm). In general, the emission of exciton is of narrow bandwidth (<50 nm).[22] With maximum emission located at 424 nm in perovskite compound **1**, the excitons have no or very little emission at 503 nm. So the presence of the excitation band of the excitons in the excitation spectrum (Figure 6c) is absolutely indicative of the occurrence of an energy transfer from the excitons to the organic ligand API·$2H^+$ in the perovskite compound **1**.

(16) (a) Chondroudis, K., Mitzi, D. B.; Brock, P. *Chem. Mater.* **2000**, *12*, 169. (b) Era, M.; Yoneda, S.; Sano, T.; Noto, M. *Thin Solid Films* **2003**, *438−439*, 322. (c) Era, M.; Miyake K.; Yoshida, Y.; Yase, K. *Thin Solid Films* **2001**, *393*, 24.

(17) (a) Ishihara, T. *J. Lumin.* **1994**, *60−61*, 269. (b) Braun, M.; Tuffentsammer, W.; Wachtel, H.; Wolf, H. C. *Chem. Phys. Lett.* **1999**, *303*, 157. (c) Papavassiliou, G. C.; Mousdis, G. A.; Koutselas, I. B. *Synth. Met.* **2001**, *121*, 1339. (d) Era, M.; Maeda, K.; Tsutsui, T. *Thin Solid Films* **1998**, *331*, 285.

(18) (a) Cheng, Z. Y.; Wang, Z.; Xing, R. B.; Han, Y. C.; Lin, J. *Chem. Phys. Lett.* **2003**, *376*, 481. (b) Cheng, Z. Y.; Shi, B. L.; Gao, B. X.; Pang, M. L.; Wang, S. Y.; Han, Y. C.; Lin, J. *Eur. J. Inorg. Chem.* **2005**, 218. (c) Braun, M.; Tuffentsammer, W.; Wachtel, H.; Wolf, H. C. *Chem. Phys. Lett.* **1999**, *307*, 373.

(19) (a) Mizukami, S.; Houjou, H.; Sugaya, K.; Koyama, E.; Tokuhisa, H.; Sasaki, T.; Kanesato, M. *Chem. Mater.* **2005**, *17*, 50. (b) Lu, W.; Chan, M. C. W.; Cheung, K. K.; Che, C. M. *Organometallics* **2001**, *20*, 2477. (c) Yoshida, K.; Ooyama, Y.; Tanikawa, S.; Watanabe, S. *J. Chem. Soc., Perkin Trans.* **20002**, 708.

(20) (a) Shi, J. M.; Xu, W.; Liu, Q. Y.; Liu, F. L.; Huang, Z. L.; Lei, H.; Yu, W. T.; Fang, Q. *Chem. Commun.* **2002**, 756. (b) Alleyne, B. D.; Hall, L. A.; Kahwa, I. A.; White, A. J. P.; Williams, D. J. *Inorg Chem.* **1999**, *38*, 6278. (c) Desiraju, G. R. *Chem. Commun.* **1997**, 1475.

(21) (a) Yu, J. H.; Lu, J.; Xu, Y.; Zhang, X.; Xu, J. Q. *Inorg. Chim. Acta*, in press. (b) Lu, J.; Zhao, K.; Fang, Q. R.; Xu, J. Q.; Yu, J. H.; Zhang, X.; Bie, H. Y.; Wang, T. G. *Cryst. Growth Des.* **2005** *5* 1091. (c) Tian, Y. Q.; Xu, L.; Cai, C. X.; Wei, J. C.; Li, Y. Z.; You, X. Z. *Eur. J. Inorg. Chem.* **2004**, 1039.

(22) Muljarov, E. A.; Tikhodeev, S. G.; Gippius, N. A.; Ishihara, T. *Phys. Rev. B* **1999**, *51*, 14370.

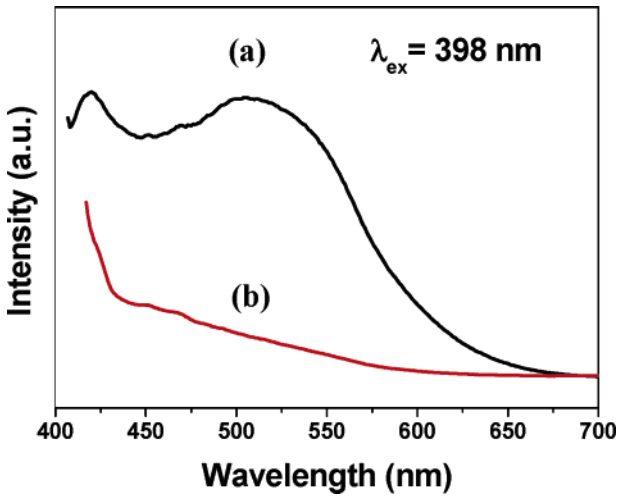

Figure 7. PL emission spectra of perovskite compound **1** (a) and API·2HBr (b) excited at 398 nm.

Under excitation into the exciton absorption at 398 nm, the obtained emission spectrum for perovskite compound **1** consists both of the emission from the exciton (424 nm) and that from the ligand (503 nm; similar to Figure 6d), but no emission is observed for the API·2HBr salt (Figure 7). This confirms the occurrence of the energy transfer from the excitons to the organic ligand in the perovskite compound **1**, which enhances the emission of the ligand API·$2H^+$ to a great extent.

To prove the proposed mechanism, the band structures of the API ligand and the perovskite were calculated using the CASTEP code based on the DFT, and exchange and correlation have been treated by generalized gradient approximation (GGA) within the scheme due to Perdew−Burke−Ernzerhof (PBE).[23] The method has been applied in some hybrid perovskites materials.[24] The calculated band structures of API·2HBr and compound **1** are given in Figure 8a,b, respectively (the calculated density of states (DOS) of the two compounds are shown in Supporting Information Figures S2 and S3, respectively). The calculated band gap is 3.8 eV for API·2HBr. The CB and VBs of the API·2HBr are primarily composed of p states associated with the mixture C 2p(π*), N 2p(π*) and C 2p(π), N 2p(π) of the imidazolium, respectively. This suggests that the luminescence of the API·2HBr arises from the $\pi-\pi$* transition. The CB of the compound **1** can be separated into two parts. The CB minimum is located at 1.0 eV as a result of the C 2p(π*) and N 2p(π*) of the imidazolium (see Figure S3, Supporting Information). The second lowest CB edges are located at 2.5−5.0 eV which is mainly composed of Pb 6p with a few contributions from the C 2p(π*) and N 2p(π*). It can be seen that the calculated ligand's band gap in compound **1** is smaller than that in free API·2HBr, indicating that formation of the perovskite lowers the π* energy of the organic molecules in the conductive band. Thus it is understandable

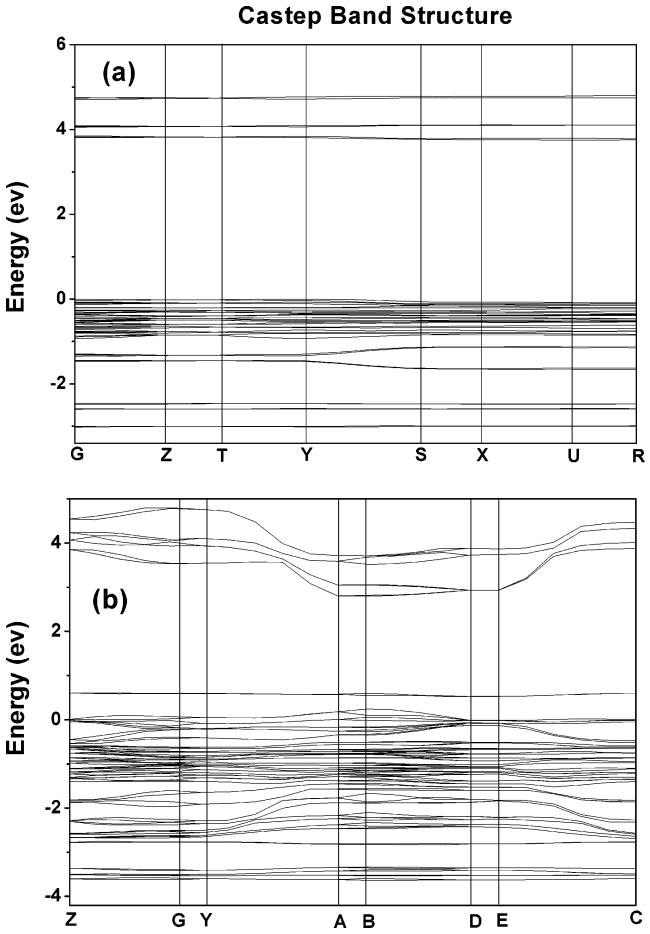

Figure 8. Calculated band structures of API·2HBr (a) and perovskite compound **1** (b).

that a red shift is observed for the emission of API·$2H^+$ in perovskite compound **1** with respect to the free API·2HBr. At the same time, the relatively low conduction of the organic molecules in the hybrid compound makes it possible for the energy transfer from the excitons to the organic ligands. It should be noted that the calculated band gaps in semiconductors may be underestimated using this first-principles energy band calculation, probably because of many factors such as the action of the crystal field, the structure model, the limits of method itself, and so forth.[25] These factors are expected to give some contributions to the change of the calculated energy level but were not included in view of the difficulty of doing so correctly. Nevertheless, the results of the calculation can well-explain the luminescence phenomenon and the proposed mechanism.

As a summary, a simple model for the luminescence and energy transfer process occurred in the organic ammonium salt API·2HBr, and the perovskite compound **1** is schematically shown in Figure 9. For the free ligand API·2HBr, upon excitation with 360 nm UV, an electron is excited from π (VB) to higher π* (CB) levels and then relaxes to the lower

(23) (a) Segall, M. D.; Lindan, P. L. D.; Probert, M. J.; Pickard, C. J.; Hasnip, P. J.; Clark, S. J.; Payne, M. C. *J. Phys.: Condens. Mater.* **2002**, 14, 2717. (b) Perdew, J. P.; Ernzerhof, B. M. *Phys. Rev. Lett.* **1996**, *77*, 3865.

(24) (a) Knutson, J. L.; Martin, J. D.; Mitzi, D. B. *Inorg. Chem.* **2005**, *44*, 4699. (b) Chang, Y. H.; Park, C. H.; Matsuishi, K. *J. Korean Phys. Soc.* **2004**, *44*, 889.

(25) (a) Fu, Z.; Zhou, S.; Zhang, S. *J. Solid State Chem.* **2005**, *178*, 230. (b) Fu, Z.; Zhou, S.; Yu, Y.; Zhang, S. *Chem. Phys. Lett.* **2004**, *395*, 285.

(26) Crystal data for compound **1**: monoclinic, space group *P*21/*c*; a = 6.1661(3) Å, b = 27.6363(12) Å, c = 8.4503(4) Å, β = 95.7120°, V = 1432.85(12) Å^3, Z = 3; T = 293 K; R1 = 0.0667 and wR2 = 0.1882; and R1 = 0.0688 and wR2 = 0.1909 (all data). CCDC 283056.

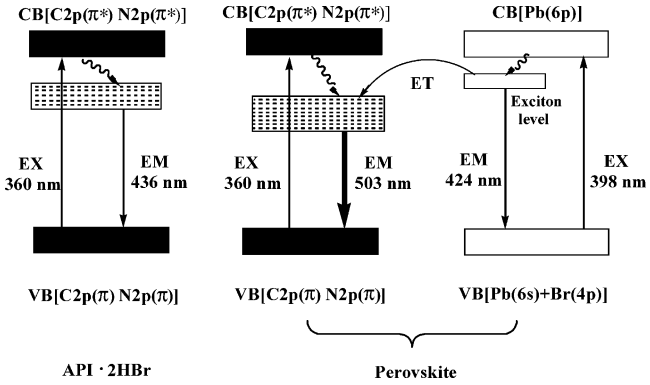

Figure 9. Schematic diagram for the luminescence and energy transfer processes that occurred in the ammonium salt API·2HBr and the perovskite compound **1** (the compositions of the VB and CB in the free ligand API·2HBr and perovskite, the $\pi-\pi^*$ transitions in API·2HBr, and the excitation and emission of the excitons together with the energy transfer from excitons to API·2HBr in the hybrid perovskite are clearly shown in the diagram; for details, see text).

π^* levels, from which it radiatively returns to the π level to produce the emission of 436 nm. In the hybrid perovskite, intermolecular interactions of the ammonium ligand lowers the $\pi-\pi^*$ transition energy and brings about the red shift for the emission of API·2HBr (503 nm). Excitation with the 398 nm UV (from VB to CB) leads to the formation of excitons in the hybrid perovskite, and the excitation energy in the excitons will release by self-emitting (at 424 nm) and transferring to the lower π^* levels of the organic molecules (API·2HBr, emitting at 503 nm) simultaneously, resulting in the totally enhanced emission intensity in the hybrid perovskite.

IV. Conclusions

Optically active organic molecules API in dication form ($API\cdot 2H^+$) interact with the $PbBr_4^{2-}$ inorganic layers through electrostatic interactions and hydrogen bonding, resulting in the formation of the rarely observed ⟨110⟩-oriented organic−inorganic perovskite structure. The optical properties (mainly emission intensity and wavelength) of the organic−inorganic perovskite compound have been improved greatly with respect to the organic ammonium salt (API·2HBr). The easy processing to even film makes this ⟨110⟩-oriented hybrid perovskite a good candidate for optoelectronic device application. The current synthetic methodology opens up possibilities for assembling novel types of hybrid perovskite through the incorporation of different types of amine into one single organic ligand, and further studies on these are in progress.

Acknowledgment. This project is financially supported by the foundation of "Bairen Jihua" of Chinese Academy of Sciences, the MOST of China (No. 2003CB314707), and National Natural Science Foundation of China (20431030, 50225205, and 00310530). The authors are very grateful to Prof. Zhijian Wu for the help in calculation.

Supporting Information Available: Crystal data of perovskite compound **1** and the free ligand API·2HBr in CIF format; crystal structure of the free ligand API·2HBr; and calculated DOS of the ligand API·2HBr and perovskite compound **1** (PDF). This material is available free of charge via the Internet at http://pubs.acs.org.

CM060714U